Gestational changes in PRMT1 expression of murine placentas

メタデータ	言語: English
	出版者:
	公開日: 2019-03-20
	キーワード (Ja):
	キーワード (En):
	作成者: 佐藤, 杏奈
	メールアドレス:
	所属:
URL	https://jair.repo.nii.ac.jp/records/2002298

1   **Gestational changes in PRMT1 expression of murine placentas**

2   Anna Sato[a, 1], Jun-Dal Kim[b], Hayase Mizukami[c], Misaki Nakashima[d], Koichiro Kako[c],

3   Junji Ishida[b], Atsuo Itakura[a], Satoru Takeda[a], Akiyoshi Fukamizu[b, *]

4

5   **Affiliations:**

6   [a]Department of Obstetrics and Gynecology, Juntendo University Faculty of Medicine, 2-

7   1-1 Hongo, Bunkyoku, Tokyo 113-8421, Japan.

8   [b]Life Science Center for Survival Dynamics, Tsukuba Advanced Research Alliance,

9   University of Tsukuba, 1-1-1 Tennodai, Tsukuba, Ibaraki 305-8577, Japan.

10 [c]Graduate School of Life and Environmental Sciences, University of Tsukuba, 1-1-1

11 Tennodai, Tsukuba, Ibaraki 305-8572, Japan.

12 [d]School of Life and Environmental Sciences, University of Tsukuba, 1-1-1 Tennodai,

13 Tsukuba, Ibaraki 305-8572, Japan.

14

15

16 *To whom correspondence should be addressed:

17 Akiyoshi Fukamizu,

18 Life science Center, Tsukuba Advanced Research Alliance,

19 University of Tsukuba, 1-1-1 Tennodai, Tsukuba, Ibaraki 305-8577, Japan.

20 Tel/Fax: (+81) 29-853-6070

21 E-mail: akif@tara.tsukuba.ac.jp.

Abstract

Introduction: In mammals, the placenta is an organ that is required to maintain the development of fetus during pregnancy. Although the proper formation of placenta is in part regulated by the post-translational modifications of proteins, little is known regarding protein arginine methylation during placental development. Here, we characterized developmental expression of protein arginine methyltransferase 1 (PRMT1) in mouse placentas.

Methods: Expression levels of PRMT1 mRNA and protein in placentas were investigated using the real-time quantitative PCR and Western blot, respectively. Next, the localization of PRMT1 was determined by immunohistochemistry and immunofluorescence analyses. In addition, the levels of methylarginines of placental proteins were quantified using liquid chromatography-tandem mass spectrometry (LC-MS/MS).

Results: PRMT1 mRNA and its protein were expressed at highest levels in mid-gestation stages, and their expression showed stepwise decrease in the late gestation. At embryonic (E) day 9, PRMT1 was observed in several different trophoblast cell (TC) subtypes. Furthermore, PRMT1 was mainly expressed in the labyrinth zone of TCs at E13. Finally, total methylarginines of proteins were significantly reduced in late gestation of placentas compared with mid-gestation stages.

Discussion: In this study, we found developmental changes in the placental expression of PRMT1 and in protein arginine methylation status during pregnancy. These findings

2

43   provide fundamental information regarding placental PRMT1-mediated arginine

44   methylation during the development.

45

46   **Keywords**: Protein arginine methyltransferase 1 (PRMT1), Placenta, Arginine

47   methylation, Methylarginines: monomethylarginine (MMA), asymmetric

48   dimethylarginine (ADMA), symmetric dimethylarginine (SDMA), Splicing variants

49

50   **1. Introduction**

51   The placenta is essential for the fetal development, forming an interface connection

52   and separating the maternal and the fetal circulations during pregnancy [1]. It is well

53   known that the fetal growth is dependent on nutrients, oxygen, metabolites, several

54   pregnancy-associated hormones, and growth factors [2]. Thus, proper formation and

55   functional maintenance of placenta are of importance for transporting these materials into

56   fetal circulation [3]. The placenta is composed of various cell types, including trophoblast

57   cells (TCs), vascular endothelial cells and blood cells, in which trophoblasts are the most

58   important for the structure and function of the placenta [4].

59   In mammals, TCs that form the outer layer of blastocyst develop into a large part of

60   the placenta and play roles either in altering maternal physiology and blood flow to

61   promote fetal growth or in nutrient uptake [3,5]. Furthermore, differentiation and

62   proliferation of TCs are accurately controlled through environmental factors and cellular

63   molecules, such as oxygen tension within the maternal–fetal interface and hormones and

64   growth factors [6]. Meanwhile, it has been reported that cellular processes of TCs, such

65 as the cell *growth*, *differentiation*, *apoptosis,* migration, and invasion are modulated by

66 transcriptional, epigenetic and metabolic regulation during placental development [7]. In

67 addition, they are generated by protein post-translational modifications (PTMs),

68 including phosphorylation, acetylation, glycosylation, ubiquitination, and lysine

69 methylation during placental development [8-11].

70 The protein arginine methylation is also one of the PTMs and is identified in arginine

71 residues of histone, transcription factors, RNA binding proteins, and signal transduction

72 factors, which are involved in various biological phenomena related to maintaining cell

73 differentiation, proliferation, growth regulation and apoptosis [12-14]. The reaction of

74 arginine methylation is catalyzed by protein arginine methyltransferases (PRMTs) that

75 form monomethylarginine (MMA), asymmetric dimethylarginine (ADMA) and

76 symmetric dimethylarginine (SDMA). Currently, nine PRMTs have been identified in

77 mammalian cells. Type I PRMTs (PRMT1, PRMT2, PRMT3, PRMT4, PRMT6, and

78 PRMT8) catalyze the formation of MMA and subsequently ADMA. PRMT5 and PRMT9,

79 as a type II PRMTs, produce SDMA via MMA, while PRMT7, a Type III PRMT, only

80 catalyze the formation of MMA [15, 16].

81 PRMT1, the most predominant of these enzymes, is responsible for over 85% of

82 cellular arginine methylation activity [17] and is ubiquitously expressed in the developing

83 embryo [18,19]. PRMT1 has two major splice variants which differ in their *N-terminus*

84 *and* in *subcellular localizations. The variant 1* is mainly localized to the nucleus and the

85 *nuclear export signal* (NES)-containing *variant* 2 is predominantly localized in the

86 cytoplasm *and may contribute to the methylation of multiple proteins. [20]*. However, the

87   physiological functions of PRMT1 have not been understood in mammals, because

88   homozygous mutant mice exhibit embryonic lethality at embryonic (E) day 6.5 [21].

89   Recently, we reported that the central nervous system (CNS)-specific PRMT1 knockout

90   mice show hypomyelination and developmental defects [22]. In addition, vascular

91   endothelial cell PRMT1-deficient mice revealed angiodysplasia that resulted in death by

92   E15 [23]. These studies indicate that PRMT1 has crucial roles in developmental stages.

93   Interestingly, it is also known that the expression level of PRMT1 in the fetus is higher

94   than in prenatal mice [21]. Thus, although it is considered that PRMT1 plays a dynamic

95   role in the development of placenta via the regulation of arginine methylation activity

96   during pregnancy, there have been no reports concerning the developmental expression

97   of PRMT1 in placenta.

98   In the present study, we found that the placental PRMT1 was highly expressed in *mid-*

99   *gestation stages.* Immunohistochemistry and immunofluorescence analyses using both a

100   LacZ-reporter-tagged heterozygous PRMT1 (*prmt1*$^{+/LacZ}$) and wild-type mice showed

101   that PRMT1 was localized in TCs or the parietal trophoblast giant cells (P-TGCs) of the

102   ectoplacental cone (EPC), the chorion and the decidua at E9, and the labyrinth-restricted

103   expression at E13. Moreover, we also found that the levels of ADMA in placental proteins

104   were comparable to the developmental expression pattern of PRMT1. Our findings

105   provide fundamental information regarding the PRMT1-mediated arginine methylation

106   during placental development.

107

108   **2. Materials and Methods**

5

109   2.1 *Antibodies*

110   The antibodies used in this study included anti-PRMT1 antibody (Millipore, 07-404),

111   anti-PRMT1 antibody (Abcam, ab92299), anti-GAPDH antibody (Cell Signaling

112   Technology, 5174), anti-rabbit IgG HRP-linked antibody (GE Healthcare, NA934), and

113   anti-rabbit IgG *biotinylated* antibody (Vector Laboratories, BA-1000).

114

115   2.2 *Animals*

116   All mice were housed under a 12 h light–12 h dark cycle, and they had free access to

117   commercial chow and filtered water. All animal experiments were carried out humanely

118   after approval from the Institutional Animal Experiment Committee of the University of

119   Tsukuba and in accordance with the Regulation of Animal Experiments of the University

120   of Tsukuba and the Fundamental Guidelines for Proper Conduct of Animal Experiments

121   and Related Activities in Academic Research Institutions under the jurisdiction of the

122   Ministry of Education, Culture, Sports, Science and Technology of Japan.

123   C57BL/6 mice were purchased from CLEA Japan (Tokyo). The $prmt1^{+/LacZ}$ knock-in

124   mice (PRMT1-KI), which carry $prmt1^{tm1a(EUCOMM)Wtsi}$ allele, were obtained from the

125   European Conditional Mouse Mutagenesis (EUCOMM). After acclimation for 7 days,

126   the mice were mated and the presence of a vaginal plug was confirmed 12–14 h later,

127   designated as embryonic day 1 (E1).

128   For genotyping PRMT1-KI mice, the tail genome DNA was isolated by the ammonium

129   acetate precipitation. Tails of mice were incubated in proteinase K at 55°C, and then

130   treated with RNase A at 37°C. Proteins were removed with 7.5 M ammonium acetate.

131   DNA was precipitated and rinsed with isopropyl alcohol and 70% ethanol. After drying,

132   DNA was dissolved in 1x Tris-EDTA buffer. Multiplex allele-specific PCR was carried

133   out with KAPA2G Robust HotStart ReadyMix with dye (Kapa Biosystems) in accordance

134   with the manufacturer's protocol using the following PCR primers: forward, 5′-

135   GTGCTTGCCATACAAGAGATCC-3′, and reverse (P1), 5′-

136   ACAGCCGAGTAGCAAGGAGG-3′, which generated 277 bp product for the *prmt1*

137   wild-type allele; and forward, 5′-ATCACGACGCGCTGTATC-3′, and reverse (P2), 5′-

138   ACATCGGGCAAATAATATCG-3′, which generated 107 bp product for the LacZ allele.

139

140   2.3 *Quantitative real-time PCR*

141   Placentas were harvested at E9, E11, E13, E16, and E19. Samples were frozen in liquid

142   nitrogen and were crushed into powder with a Multi-beads Shocker (Yasui Kikai Co.,

143   Osaka, Japan). Total RNA was extracted using ISOGEN II (Nippon Gene Co.).

144   Complementary DNA (cDNA) was synthesized from total RNA with Random Hexamer

145   Primer (Roche) using ReverTra Ace qPCR RT Master Mix (TOYOBO). Quantitation of

146   gene expression was assessed using real-time PCR with SYBR Green PCR Master Mix

147   and the Thermal Cycler Dice Real Time System (Takara BIO Inc.). PCR cycling

148   conditions were 95°C for 30 s, followed by 40 cycles of 95°C for 5 s, 60°C for 30 s, and

149   then 95°C for 15 s and 60°C for 30 s, and finally 95°C for 15 s. Results were normalized

150   to the *gapdh* as a housekeeping gene, and the $\Delta\Delta C$t method was used for all real-time

151   PCR analyses. Amplifications were done as technical duplicates. Primer sequences are

152   given in Supplementary Table 1.

153

154 2.4 *Western blot*

155   The tissue powder was resuspended in 25 μL of lysis buffer (20 mM Tris-HCl [pH 7.4]

156 150 mM NaCl, 5 mM EDTA, pH 8.0, 1% Nonidet P-40, 5% glycerol, and 1x protease

157 inhibitor cocktail) and then was lysed using a bath-type sonicator (Cosmobio, Bioruptor

158 UCD-250). Tissue and cell debris were removed by centrifugation at 14,000 rpm at 4°C

159 for 10 min. Supernatants were mixed with 25 µL of 2x Laemmli sample buffer (Bio-Rad)

160 and heated at 95°C for 5 min. Subsequently, samples were resolved using 10% SDS-

161 PAGE and transferred to polyvinylidene difluoride (PVDF) membranes. The membranes

162 were incubated with the appropriate primary and secondary antibodies at 4˚C overnight.

163 Protein bands were detected using Luminata Forte Western HRP substrate (Millipore)

164 and exposed to X-ray film (Fujifilm).

165

166 2.5 *β-galactosidase staining*

167   Placentas of PRMT1-KI mice were harvested at E9 and E13, and perfused with 4%

168 paraformaldehyde and fixed for 15 min. Tissues were embedded in OCT compound, and

169 then they were sectioned into 10 μm thickness using a rotary microtome (HM560;

170 Microm Cryostat, Thermo Scientific). Sections were incubated in X-Gal staining solution

171 (1 mg/ml X-Gal, 5 mM potassium ferrocyanide, 5 mM potassium ferricyanide, 2 mM

172 $MgCl_2$, 0.02% NP-40 and 0.05% sodium deoxycholate in phosphate buffered saline

173 (PBS)) at 37°C overnight. After eosin staining, samples were washed three times in PBS

174 buffer.

175

176 2.6 *Immunofluorescence*

177   Placentas of C57BL/6 mice were harvested at E9 and E13, and perfused with 4%

178 paraformaldehyde and fixed overnight. Samples were embedded in paraffin, and then

179 were sectioned into 8-μm thickness using a rotary microtome (Microm International

180 GmbH). They were deparaffinized following antigen retrieval in heated citrate buffer (pH

181 6.0), and then incubated with PBS buffer containing 5% bovine serum albumin (BSA)

182 and 0.05% Tween-20. Next, sections were washed in PBS buffer, and then were incubated

183 with anti-PRMT1 antibody at 4 °C overnight. Samples were washed and incubated with

184 the biotinylated secondary antibody for 1 h, followed by the streptavidin conjugated to

185 Alexa Fluor 647 dye (Thermo Fisher Scientific, S21374) at room temperature for 90 min.

186 For quenching the lipofuscin, samples were treated with TrueBlack Lipofuscin

187 Autofluorescence Quencher reagent (Biotium) at room temperature for 1 min, and then

188 they were washed in PBS. To visualize the nuclei, they were stained with Hoechst 33258,

189 and a confocal laser-scanning microscope (Fluoview FV10i, Olympus) was used to obtain

190 fluorescence images.

191

192 2.7 *Quantification of methylarginines by liquid chromatography-tandem mass*

193 *spectrometry (LC-MS/MS)*

194   Approximately 50 mg of the placental powder was suspended in 200 μL of HPLC-

195 grade water (Wako Pure Chemicals) and homogenized using a bath-type sonicator

196 (Cosmobio, Bioruptor UCD-250). The extract was centrifuged at 14,000 rpm for 15 min

197   at 4 °C, and insoluble matters was removed. The protein concentration of the supernatant

198   (150 μL) was determined by Bio-Rad DC protein assay (Bio-Rad) in accordance with a

199   modified Lowry's method [24]. Methanol (400 μL) was added to 100 μL of the sample

200   (including 100 μg of proteins), and the mixture was vigorously mixed. Chloroform (100

201   μL) was then added, and also mixed. The mixture was further mixed with 300 μL of

202   HPLC-grade water, followed by centrifugation at 14,000 rpm for 1 min. The

203   water/methanol layer was removed and proteins remained at the phase boundary between

204   the water/methanol and the chloroform layers. After 400 μL of methanol were added to

205   the sample and the mixture was gently mixed, the sample was spun at 14,000 rpm for 10

206   min. The supernatant was carefully removed and the pellet was dried up *in vacuo*. The

207   dried protein pellet was dissolved with 100 μL of 6N HCl (Wako Pure Chemicals) and

208   spiked with 5 μL of 23.2 μM *N*-propyl-L-arginine (N-PLA, Abcam). After the hydrolysis

209   at 110 °C for 24 h, the sample was subsequently dried with a vacuum centrifuge. The

210   residue was reconstituted with 50 μL of HPLC-grade water by vortexing, and centrifuged

211   at 14,000 rpm for 15 min. Ten-times diluent of the supernatant (1 or 2.5 μL) was injected

212   into LC-MS/MS. The LC-MS/MS analysis was performed on a Shimadzu LCMS-8050

213   triple quadrupole mass spectrometer coupled with a Shimadzu Nexera X2 ultra-high

214   pressure liquid chromatography (UHPLC) system (Shimadzu). SeQuant ™ ZIC-HILIC

215   ™ column (2.1 × 150 mm, Merck KGaA) with a SeQuant ™ ZIC-HILIC ™ Guard Fitting

216   (1.0 × 14 mm, Merck KGaA) was used as a separation column unit of LC part. The LC

217   separation and the MS operation was carried out as previously described in [25]. All

218   analyses and data processing were completed using the Lab-Solutions V5.60 software

219   (Shimadzu Scientific Instruments, Inc.).

220

221   2.8 *Statistical analysis*

222   The results were presented as the mean ± SEM. Differences between groups were

223   analyzed by using the ANOVA test followed by Dunnett's multiple comparison test or

224   the two-tailed Student *t*-test in Prism 5.0 or 6.0 software, using a significance index of

225    $P < 0.05$ and $P < 0.0001$.

226

227   **3. Results**

228   3.1 *Changes in placental PRMT1 expression during the gestational period.*

229   We characterized the expression profiles of PRMT1 mRNAs and proteins in mouse

230   placentas at E9, E11, E13, E16, and E19. As shown in Figure 1A, PRMT1 mRNAs were

231   highly expressed in *mid-gestation stages* (E9, E11 and E13), compared to late stages of

232   pregnancy (E16 and E19). Next, we evaluated the expression of PRMT1 proteins by

233   Western blotting and revealed that the levels of PRMT1 variant 1 (v1) were also increased

234   from E9 to E13, and decreased starting at E16. By contrast, variant 2 (v2) levels were

235   increased in placentas from E13 to E19. These results suggested that the expression of

236   placental PRMT1 variants is regulated in a gestational age-dependent manner (Fig. 1B).

237

238   3.2 *Identification of prmt1 promoter activity in the placenta.*

11

239   We have previously reported the roles of PRMT1 in CNS development and embryonic

240   vascular formation through analysis of CNS- and endothelial-specific PRMT1 knock-out

241   mice, respectively [22,23], which were originally generated from *prmt1* promoter-driven

242   bacterial β-galactosidase reporter gene (LacZ) knocked in mice (*prmt1*[+/LacZ]; PRMT1 KI)

243   (Fig. 2A, B). Our PRMT1 KI mice are useful to visualize the prmt1 promoter activity via

244   the β-galactosidase activity. As shown in Figure 2C, X-Gal staining in PRMT1 KI mice

245   displayed high constitutive activity driven by the prmt1 promoter in mouse placental cells,

246   with strong signals in the ectoplacental cone (EPC), the chorion, the parietal trophoblast

247   giant cells (P-TGC) and the antimesometrial decidua (AD) areas at E9.

248   In the mature placenta, the labyrinth contains the maternal-fetus vasculature for the

249   exchange of nutrients and wastes, while the junctional zone (Jz) is proximal to maternal

250   tissues and has a primary endocrine role [26]. Therefore, we evaluated the β-galactosidase

251   activity in *mid-gestation stage* (E13) and found *prmt1* promoter-driven β-galactosidase

252   activity was widely observed in P-TGCs, TCs of the junctional and the labyrinth zones.

253   In contrast, they were not detected in the decidua (De) (Fig. 2D).

254

255   3.3 *Region-restricted localization of endogenous PRMT1 in the placenta.*

256   Next, to determine the expression site of endogenous PRMT1 proteins in placentas at

257   E9 and E13, we performed immunofluorescence analysis with anti-PRMT1 antibody.

258   *Lipofuscin*, *a yellow-brown pigment*, causes autofluorescence, leading to low-quality

259   images that impair assessment in tissue sections [27,28]. Moreover, it is known that auto-

260   fluorescent lipofuscin granules are increased in the *placenta* at mid-gestation stages [29].

261 Therefore, we used a combined method based on quenching for the lipofuscin

262 autofluorescence [30] and long-wavelength fluorescent probe-conjugated secondary

263 antibody. *First*, we confirmed the reduced autofluorescence in the placental section with

264 the quenching of lipofuscin (Supplementary figure 1). The use of anti-PRMT1 antibody

265 in fluorescence images showed the *expression of* PRMT1 in P-TGCs, TCs of EPC and

266 chorion: they were localized to the nucleus at E9, but not the AD areas-enriched cells

267 (Fig. 3A and B). Further, at E13, the placental section revealed that endogenous PRMT1

268 was *predominantly* expressed in the cytoplasm of labyrinth zone cells (Fig. 3C and D).

269 By contrast, they were not detected in the Jz.

270

271 3.4 *Placental ADMA levels.*

272   Finally, to determine whether the ontogenic change in PRMT1 expression contributes

273 to arginine methylation of overall placental protein, liquid chromatography-tandem mass

274 spectrometry (LC-MS/MS) analysis was used to quantify the amounts of MMA and

275 ADMA, which are catalyzed by Type I PRMTs in the acid hydrolyzed placental proteins

276 at E9, E11, E13, E16, and E19. We have recently optimized the condition for multiple

277 reaction monitoring (MRM) to measure methylarginines such as MMA, ADMA and

278 SDMA from animal tissue samples using LC-MS/MS [22,25]. As shown in Figure 4A,

279 we confirmed the elution time of MMA and ADMA from placental proteins at 10.51 min

280 and 10.31 min, respectively. Whereas MMA levels in placental proteins were not

281 significantly changed during pregnancy, amounts of placental ADMA showed highest

282 levels at E11, and they then showed decrease in the late gestation (Fig. 4B). These results

13

283 suggested that both PRMT1 expression and ADMA levels were parallel at each

284 gestational period.

285

286 **4. Discussion**

287 Protein arginine methylation is found on *various intracellular proteins, and is*

288 *catalyzed by* a family of nine PRMTs in mammals [14-16]. The expression of placental

289 PRMTs mRNAs showed ontogenic changes during pregnancy, in which there had

290 different patterns among PRMTs (Fig. 1A and Supplementary figure 2), suggesting they

291 play roles in a variety of *cellular processe*s. PRMT1 is known to methylate histone and

292 various non-histone proteins that are involved in the regulation of cellular functions, and

293 is also required for mammalian development and survival [31]. It is reported that

294 the human PRMT1 was alternatively spliced to yield seven isoforms with distinct N-

295 terminal sequences, in which both *variants* 1 and 2 are often expressed in mammalian

296 cells [20]. Importantly, we determined stepwise decrease in the placental PRMT1 variant

297 1 expression and a *sequential* increase in its variant 2 from E13 (Fig. 1B). As shown in

298 Figure 3B, PRMT1 was exclusively expressed in the nucleus at E9. Furthermore, at E13,

299 PRMT1 showed cytoplasmic and region-restricted localization in the labyrinth zone (Fig.

300 3D). These results indicate that the differential *alternative splicing* of placental PRMT1

301 leads to change the balance of protein methylation between the *nucleus* and *cytoplasm i*n

302 a gestational age-dependent manner.

303 At E11 to E13, with higher expression of PRMT1, the placental structure is changed,

304 causing the general shape of the decidua basalis, Jz and the membranous labyrinth to have

14

305 completed in mice [1,3,32]. Moreover, at this stage, the placental labyrinth is important

306 for maternal and fetal circulations, hence its proper formation is essential for

307 embryogenesis. Although the function of Jz in mice is still largely unknown, it has been

308 shown to support the labyrinth development in areas such as growth and expansion [1].

309 On the other hand, despite the fact that the promoter activity of *Prmt1* gene was observed

310 in TCs of the Jz at E13 (Fig. 2D), PRMT1 proteins were not detected (Fig. 3D). The

311 trophoblast-specific protein alpha (*Tpbpa*) gene is a marker of spongiotrophoblast and

312 glycogen TCs in the Jz [33]. Considering the role of PRMT1 in the Jz, we generated the

313 junctional trophoblast-specific *Prmt1*-knockout (*Tpbpa-Cre:Prmt1* KO) mice lacking

314 exons 4 and 5, which encode a part of the methyl-donor binding domain [15] by mating

315 *Prmt1$^{flox/flox}$* mice with *Tpbpa-Cre* transgenic mice [34] (Supplementary figure 3).

316 However, the morphological characteristics of placenta were not significantly different

317 between *Tpbpa-Cre: Prmt1* KO mice and controls at E14 or E19 (Supplementary figure

318 4). Furthermore, *Tpbpa-Cre:Prmt1* KO fetuses were born, and also showed normal

319 growth (Supplementary figure 5), suggesting *the dispensable role of* PRMT1 in the

320 formation and the function of Jz.

321   It is known that the ADMA is produced during proteolysis, and inhibits nitric oxide

322 synthase [35,36]. Nitric oxide (NO), a potent vasodilator, modulates the fetoplacental

323 vascular reactivity, vascular resistance in the placental bed, invasion of trophoblasts, and

324 adhesion and aggregation of platelets [37-40]. In addition, NO plays a role in epigenetic

325 fetal programming via the chromatin modification [41-43]. In a normal pregnancy, the

326 level of plasma ADMA is reduced with increasing gestational age [35]. Notably, placental

327 ADMA levels also showed an ontogenic decrease in parallel with PRMT1 expression

328 changes in gestation (Fig. 1B, 4B). Thus, these findings suggest that PRMT1 is involved

329 in the modulation of the ADMA-mediated NO synthase pathway during pregnancy.

330 A previous report identified lethality of conventional PRMT1 knockout mice in the

331 early stage of embryonic development [21]. More recently, our studies and those of other

332 groups have found important roles of PRMT1 in the central nervous system, embryonic

333 angiogenesis, muscle regeneration and innate immune response using cell type-specific

334 knockout mouse models [22,23,44,45]. Importantly, these *in vivo* studies suggest that

335 PRMT1 is crucial for prenatal and neonatal development, and postnatal maintenance of

336 functions. While the physiological role of PRMT1 is being analyzed in fetuses at perinatal

337 stages, the role(s) of PRMT1 was poorly understood in the placenta. Therefore, this study

338 is the first to investigate placental PRMT1 expression profile in the gestational period,

339 and will serve as a reference database to gain insight into the maintenance of maternal

340 and fetal homeostasis with the PRMT1-mediated protein arginine methylation.

341

347

348 **Conflict of interest**

16

349   The authors declare that they have no conflicts interest.

350

357

358   **References**

359   [1] J. Rossant, J.C. Cross, Placental development: Lessons from mouse mutants, Nat. Rev.

360   Genet. 2 (2001) 538-546.

361   [2] K.E. Brett, Z.M. Ferraro, J. Yockell-Lelievre, A. Gruslin, K.B. Adamo, Maternal-fetal

362   nutrient transport in pregnancy pathologies: the role of the placenta, Int. J. Mol. Sci.

363   15 (2014) 16153-16185.

364   [3] E.D. Watson, J.C. Cross, Development of structures and transport functions in the

365   mouse placenta, Physiology 20 (2005) 180-193.

366   [4] J.C. Cross, How to make a placenta: mechanisms of trophoblast cell differentiation in

367   mice--a review, Placenta 26 (Suppl A) (2005) S3-9.

368   [5] K. Ogura, M. Sakata, M. Yamaguci, M. Kurachi, Y. Murata, High concentration of

369   glucose decreases glucose transporter-1 expression in mouse placenta *in vitro* and *in*

370   *vivo*, J. Endocrinol. 160 (1999) 443-452.

371 [6] K. Red-Horse, Y. Zhou, O. Genbacev, A. Prakobphol, R. Foulk, M. McMaster, S.J.

372   Fisher, Trophoblast differentiation during embryo implantation and formation of the

373   maternal-fetal interface, J. Clin. Invest. 114 (2002) 744-754.

374 [7] E. Maltepe, A.I. Bakardjiev, S.J. Fisher, The placenta: transcriptional, epigenetic, and

375   physiological integration during development, J. Clin. Invest. 120 (2010) 1016-1025.

376 [8] T.D. Burrows, A. King, S.K. Smith, Y.W. Loke, Human trophoblast adhesion to

377   matrix proteins: inhibition and signal transduction, Hum. Reprod. 10 (1995) 2489-

378   2500.

379 [9] H.R. Kohan-Ghadr, L. Kadam, C. Jain, D.R. Armant, S. Drewlo, Potential role of

380   epigenetic mechanisms in regulation of trophoblast differentiation, migration, and

381   invasion in the human placenta, Cell Adh. Migr. 10 (2016) 126-135.

382 [10] Q. Chen, P.C. Pang, M.E. Cohen, M.S. Longtine, D.J. Schust, S.M. Haslam, S.M.

383   Blois, A. Dell, G.F. Clark, Evidence for differential glycosylation of trophoblast cell

384   types, Mol. Cell Proteomics 15 (2006) 1857-1866.

385 [11] W.H. Townley-Tilson, Y. Wu, J.E. 3rd Ferguson, C. Patterson, The ubiquitin ligase

386   ASB4 promotes trophoblast differentiation through the degradation of ID2, PloS One

387   9 (2014) e89451.

388 [12] Y.H. Lee, M.R. Stallcup, Minireview: protein arginine methylation of nonhistone

389   proteins in transcriptional regulation, Mol. Endocrinol. 23 (2009) 425-433.

390 [13] Y.Yang, M.T. Bedford, Protein arginine methyltransferases and cancer, Nat. Rev.

391   Cancer 13 (2013) 37-50.

392　[14] M.T. Bedford, S. Richard, Arginine methylation an emerging regulator of protein

393　　　function, Mol. Cell 18 (2005) 263-272.

394　[15] M.T. Bedford, S.G. Clarke, Protein arginine methylation in mammals: who, what,

395　　　and why. Mol. Cell 33 (2009) 1-13.

396　[16] R. Blanc, S. Richard, Arginine methylation: The coming of age, Mol. Cell 65 (2017)

397　　　8-24.

398　[17] O. Obianyo, C.P. Causey, J.E. Jones, P.R. Thompson, Activity-based protein

399　　　profiling of protein arginine methyltransferase 1, ACS Chem. Biol. 6 (2011) 1127-

400　　　1135.

401　[18] H.S. Scott, S.E. Antonarakis, M.D. Lalioti, C. Rossier, P.A. Silver, M.F. Henry,

402　　　Identification and characterization of two putative human arginine

403　　　methyltransferases (HRMT1L1 and HRMT1L2), Genomics 48 (1998) 330-340.

404　[19] E. Hong, Y. Lim, M. Oh, D. Kwon, Tissue-specific and age-dependent expression

405　　　of protein arginine methyltransferases (PRMTs) in male rat tissues, Biogerontology

406　　　13 (2012) 329-336.

407　[20] I. Goulet, G. Gauvin, S. Boisvenue, J. Côté,

408　　　Alternative splicing yields protein arginine methyltransferase 1 isoforms with distin

409　　　ct activity, substrate specificity, and subcellular localization, J. Biol. Chem. 282

410　　　(2007) 33009-33031.

411　[21] M.R. Pawlak, C.A. Scherer, J. Chen, M.J. Roshon, H.E. Ruley, Arginine N-

412　　　methyltransferase 1 is required for early postimplantation mouse development, but

413　　　cells deficient in the enzyme are viable, Mol. Cell. Biol. 20 (2000) 4859-4869.

414 [22] M. Hashimoto, K. Murata, J. Ishida, A. Kanou, Y. Kasuya, A. Fukamizu, Severe

415 hypomyelination and developmental defects are caused in mice lacking protein

416 arginine methyltransferase 1 (PRMT1) in the central nervous system, J. Biol. Chem.

417 291 (2016) 2237-2245.

418 [23] T. Ishimaru, J. Ishida, J.D. Kim, H. Mizukami, K. Hara, M. Hashimoto, K. Yagami,

419 F. Sugiyama, A. Fukamizu, Angiodysplasia in embryo lacking protein arginine

420 methyltransferase 1 in vascular endothelial cells, J. Biochem. 161 (2017) 255-258.

421 [24] O.H. Lowry, N.J. Rosebrough, A.L. Farr, R.J. Randall, Protein measurement with

422 the Folin phenol reagent, J. Biol. Chem. 193 (1951) 265-275.

423 [25] A. Kanou, K. Kako, K. Hirota, A. Fukamizu, PRMT-5 converts

424 monomethylarginines into symmetrical dimethylarginines in Caenorhabditis elegans,

425 J. Biochem. 161 (2017) 231-235.

426 [26] J.F. Silva, R. Serakides, Intrauterine trophoblast migration: A comparative view of

427 humans and rodents, Cell Adh. Migr. 10 (2016) 88-110.

428 [27] F.C. Delori, C.K. Dorey, G. Staurenghi, O. Arend, D.G. Goger, J.J. Weiter, In vivo

429 fluorescence of the ocular fundus exhibits retinal pigment epithelium lipofuscin

430 characteristics, Invest. Ophthalmol. Vis. Sci. 36 (1995) 718-729.

431 [28] Y. Sun, A. Chakrabartty, Cost-effective elimination of lipofuscin fluorescence from

432 formalin-fixed brain tissue by white phosphor light emitting diode array, Biochem.

433 Cell Biol. 94 (2016) 545-550.

434 [29] A.M. Brown, H.E. Enesco, Lipofuscin in mouse placenta: Variations with age, AGE

435 7 (1984) 36-41.

436   [30] J. Yang, F. Yang, L.S. Campos, W. Mansfield, H. Skelton, Y. Hooks, P. Liu,

437   Quenching autofluorescence in tissue immunofluorescence, Mol. Cell. Biol. 29

438   (2009) 2982-2996.

439   [31] Z. Yu, T. Chen, J. Hébert, E. Li, S. Richard, A mouse PRMT1 null allele defines an

440   essential role for arginine methylation in genome maintenance and cell proliferation,

441   Wellcome Open Res. 2:79 (2017) DOI 10.17605/OSF.IO/3E4KV.

442   [32] A. Malassiné, J.L. Fredo, D. Evain-Brion, A comparison of placental

443   development and endocrine functions between the human and mouse model, Hum.

444   Reprod. Update. 9 (2003) 531-539.

445   [33] N. Sharma, C. Kubaczka, S. Kaiser, D. Nettersheim, S.S. Mughal, S. Riesenberg,

446   M. Hölzel, E. Winterhager, H. Schorle, Tpbpa-Cre-mediated deletion of TFAP2C

447   leads to deregulation of Cdkn1a, Akt1 and the ERK pathway, causing placental

448   growth arrest, Development 144 (2017) 3731-3743.

449   [34] D.G. Simmons, A.L. Fortier, J.C. Cross, Diverse subtypes and developmental origins

450   of trophoblast giant cells in the mouse placenta, Dev. Biol. 304 (2007) 567-578.

451   [35] L.T. Huang, C.S. Hsieh, K.A. Chang, Y.L. Tain, Roles of nitric oxide and

452   asymmetric dimethylarginine in pregnancy and fetal programming, Int. J. Mol. Sci.

453   13 (2012) 14606-14622.

454   [36] M.D. Savvidou, A.D. Hingorani, D. Tsuikas, J.C. Frölich, P. Vallance, K.H.

455   Nicolaides, Endothelial dysfunction and raised plasma concentrations of asymmetric

456   dimethylarginine in pregnant women who subsequently develop pre-eclampsia,

457   Lancet. 361 (2003) 1511-1517.

458   [37] S.M. Sladek, R.R. Magness, K.P. Conrad, Nitric oxide and pregnancy, Am. J.

459   Physiol. 272 (1997) R441-463.

460   [38] B.J. Krause, M.A. Hanson, P. Casanello, Role of nitric oxide in placental vascular

461   development and function, Int. J. Mol. Sci. 13 (2012) 14606-14622.

462   [39] H. Maul, M. Longo, G.R. Saade, R.E. Garfield, Nitric oxide and its role during

463   pregnancy: from ovulation to delivery, Curr. Pharm. Des. 9 (2003) 359-380.

464   [40] F. Lyall, I.A. Greer, A. Young, L. Myatt, Nitric oxide concentrations are increased

465   in the feto-placental circulation in intrauterine growth restriction, Placenta 17 (1996)

466   165-168.

467   [41] X.F. Xu, X.L. Ma, Z. Shen, X.L. Wu, F. Cheng, L.Z. Du, Epigenetic regulation of

468   the endothelial nitric oxide synthase gene in persistent pulmonary hypertension of

469   the newborn rat, J. Hypertens. 28 (2010) 2227-2235.

470   [42] B. Illi, C. Colussi, A. Grasselli, A. Farsetti, M.C. Capogrossi, C. Gaetano, NO sparks

471   off chromatin: Tales of a multifaceted epigenetic regulator, Pharmacol. Ther 123

472   (2009) 344-352.

473   [43] A. Nott, A. Riccio, Nitric oxide-mediated epigenetic mechanisms in developing

474   neurons, Cell Cycle 8 (2009) 725-730.

475   [44] R.S. Blanc, G. Vogel, X. Li, Z. Yu, S. Li, S. Richard, Arginine methylation by

476   PRMT1 regulates muscle stem cell fate, Mol. Cell. Biol. 37 (2017) e00457-16.

477 [45] I. Tikhanovich, J. Zhao, J. Olson, A. Adams, R. Taylor, B. Bridges, L. Marshall, B.

478 Roberts, S.A. Weinman, Protein arginine methyltransferase 1 modulates innate

479 immune responses through regulation of peroxisome proliferator-activated receptor

480 γ-dependent macrophage differentiation, Placenta 32 (2011) 797-805.
481

482 **Figure legends**

483 **Fig. 1. Altered placental PRMT1 expression in different gestational stages.** (**A**)

484 Quantitative real-time PCR analysis for relative mRNA expression of *prmt1* in the

485 placentas (*n* = 5 per gestational stage, E9, 11, 13, 16 and 19). (**B**) Representative Western

486 blots demonstrating the ontogenic decrease in PRMT1 expression, with GAPDH shown

487 as a loading control. Arrowheads indicate variant 1 (v1) and variant 2 (v2).

488

489 **Fig. 2. Identification of the *prmt1* promoter-driven β-galactosidase activity at E9 and**

490 **13.** (**A**) Generation of *prmt1*$^{+/\text{LacZ}}$ knock-in (KI) mice by gene targeting: schematic

491 representation of the targeting strategy used to knock-in a LacZ cassette into the mouse

492 *prmt1* locus. Exons are indicated by open box with exon numbers. Arrows indicate the

493 positions of the P1, P2, P3 and P4 genotyping primers. (**B**) Allele-specific PCR analysis

494 for genotyping *prmt1*$^{\text{wt}}$ and *prmt1*$^{+/\text{LacZ}}$ mouse lines using tail genomic DNA. Products of

495 277 and 107 base pairs (bp) were generated from *prmt1*$^{\text{wt}}$ and *prmt1*$^{+/\text{LacZ}}$ mice,

496 respectively. (**C**) Left panel: Representative sagittal sections of LacZ (β-galactosidase

497 activity) and eosin stained in E9 placenta (scale bar, 500 μm). Bottom and Right panels:

498 Enlarged images of the boxed areas with LacZ-positive cells (scale bars, 50 μm). EPC,

499   ectoplacental cone; Ch, chorion; Em, embryo; De, decidua; EC, ectoplacental cavity; P-

500   TGC (arrow heads), parietal trophoblast giant cell; Amn, amnion; AD, antimesometrial

501   decidua; UL, uterine lumen. (**D**) Top panel: Representative sagittal sections of LacZ (β-

502   galactosidase activity) and eosin stained in E13 placenta (scale bar, 500 μm). Bottom

503   panels: Enlarged images of the boxed areas with LacZ-positive cells (scale bars, 50 μm).

504   De, decidua; Jz, junctional zone; La, labyrinth.

505

506   **Fig. 3. Immunohistochemical localization of endogenous PRMT1 in the placenta at**

507   **E9 and E13.** (**A**) Schematic representation of main structure of an E9 mouse placenta.

508   EPC, ectoplacental cone; Ch, chorion; De, decidua; EC, ectoplacental cavity; P-TGC,

509   parietal trophoblast giant cell; AD, antimesometrial decidua. (**B**) Enlarged images of the

510   boxed areas in (A). Representative confocal images of PRMT1-positive cells (magenta)

511   in placenta areas at E9. Hoechst 33258 staining (blue) was performed to visualize cell

512   nuclei. (**C**) Schematic representation of main structure of an E13 mouse placenta. Jz,

513   junctional zone; La, labyrinth. (**D**) Enlarged images of the boxed areas in (C). Confocal

514   images of PRMT1-positive cells in the labyrinth zone at E13. Scale bars, 20 μm.

515

516   **Fig. 4. Quantification of MMA and ADMA levels in protein hydrolysates of**

517   **placentas.** (**A**) Representative mass chromatograms of placental MMA (left panels) and

518   ADMA (right panels) at E9, E11, E13, E16, and E19. Conditions and detailed data are

519   described in "**Materials and Methods**" and [25]. (**B**) Amounts of MMA and ADMA in

520   placentas as pmol per 100 μg protein. Results are given as the mean ± SEM of n = 5

521   independent experiments; $*P < 0.05$ and $***P < 0.0001$ and ns (not significant), each

522   stage versus E11 (one-way ANOVA followed by Dunnett's multiple comparison test).
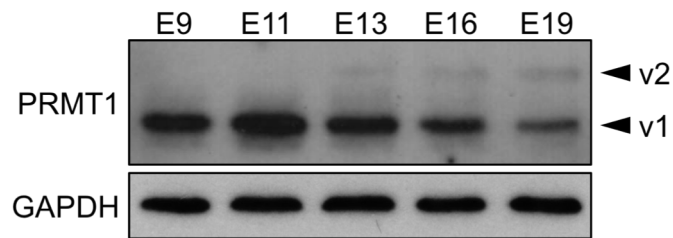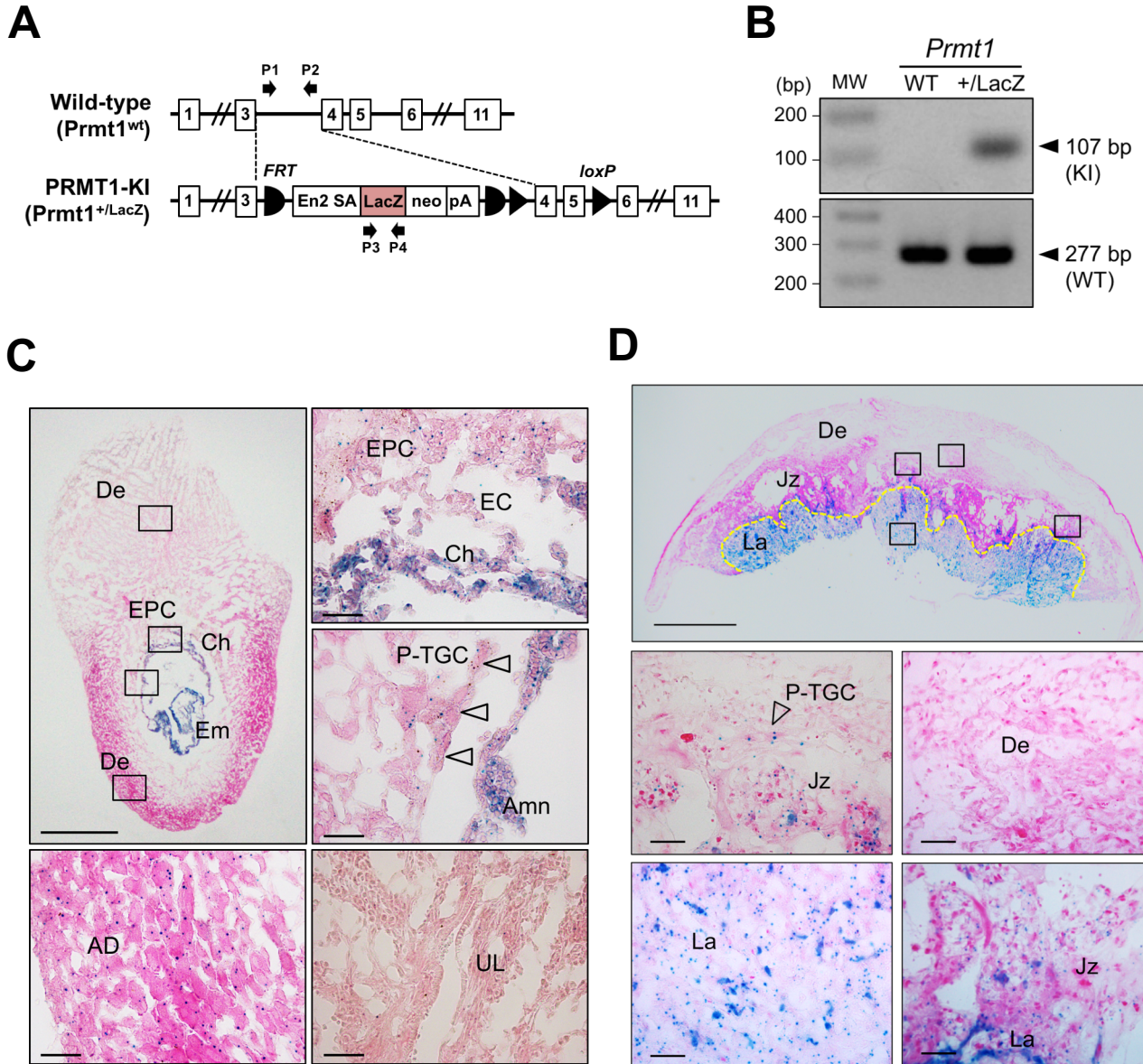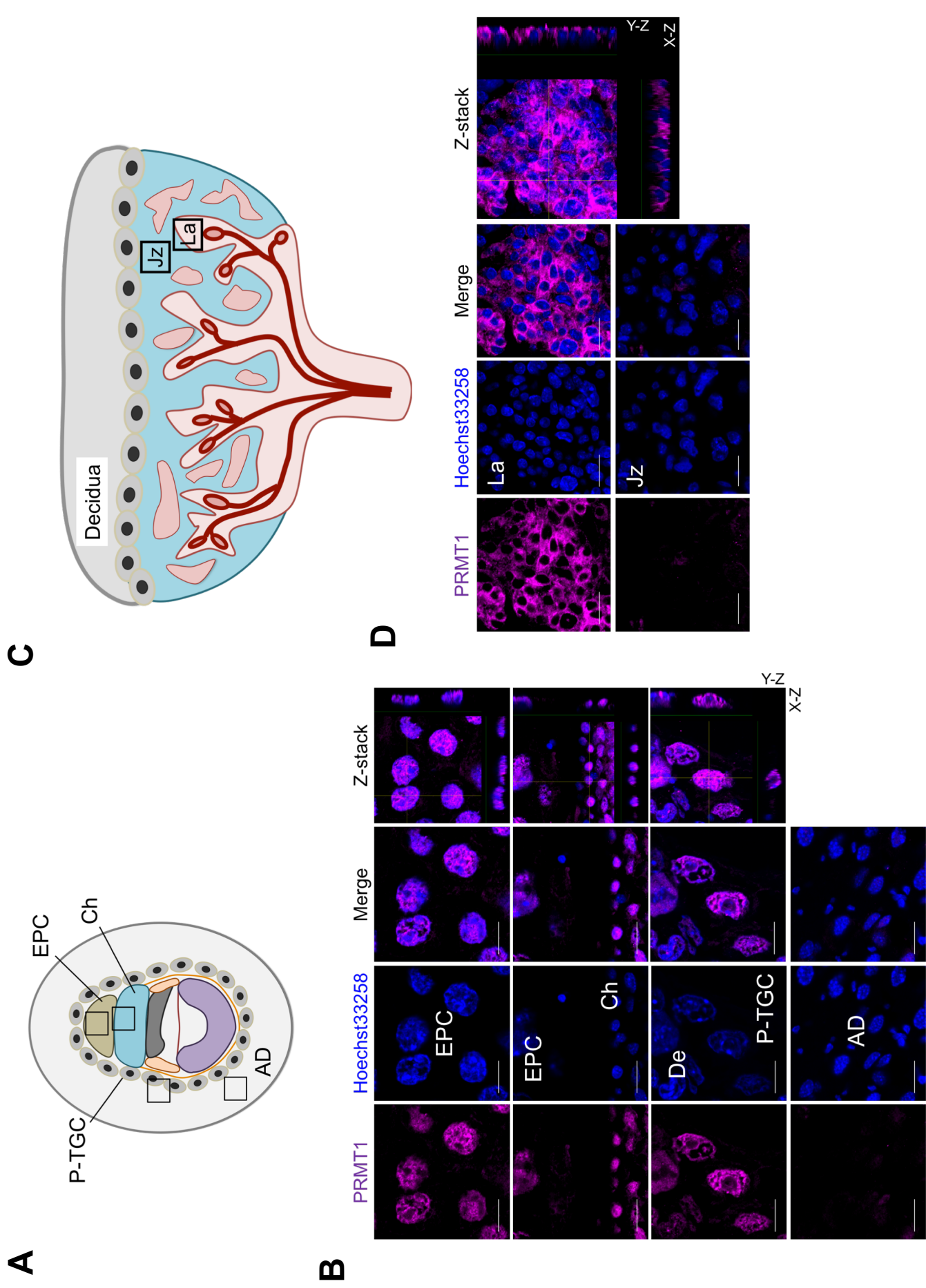
Figure 1

Figure 2

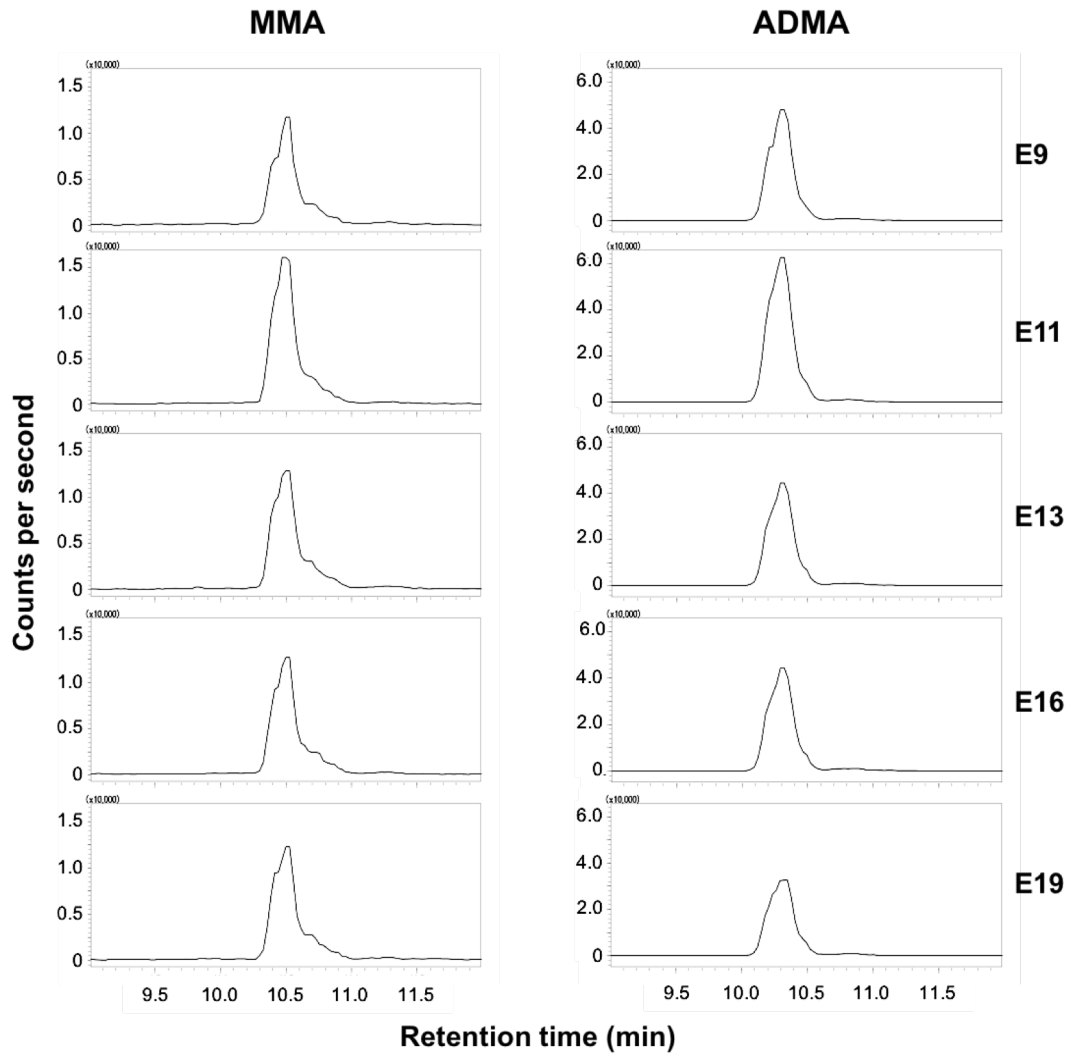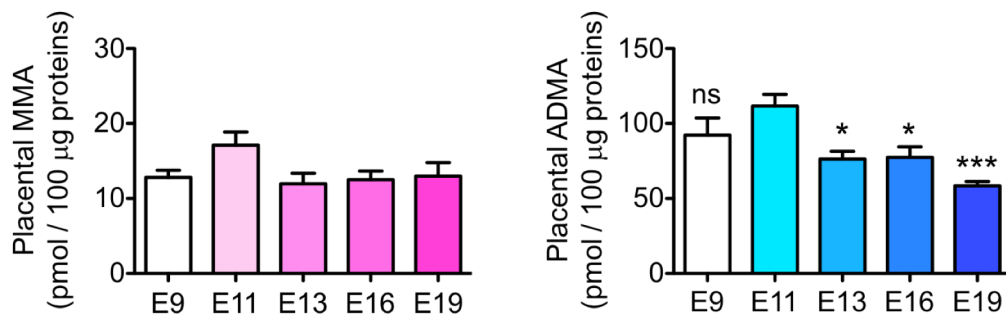**A**

B

C

D

Figure 3

Figure 4

A
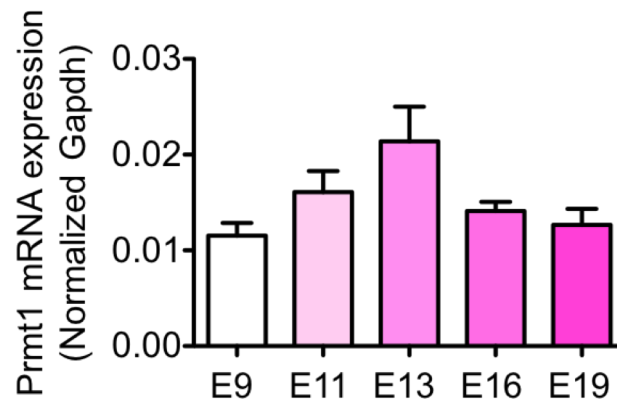
Supplementary material

S1. Materials and Methods

S1.1 *Generation of the junctional trophoblast-specific Prmt1-knockout mice* (*Tpbpa-Cre*:*Prmt1* KO)

Prmt1^{flox/flox} (*Prmt1^{ff}*) mice were established as previously reported (Ref. 22), which were mated with *Tpbpa-Cre* transgenic mice [Tg(Tpbpa-cre,-EGFP)5Jcc], Common Name: 4311-Cre, Canadian Mouse Mutant Repository) to create *Tpbpa-Cre*:*Prmt1^{-/-}* mice.

S1.2 *Genotyping*

PCR amplification of *Prmt1* was performed using the following PCR primers: forward primer (P1) 5'-GTGCTTGCCATACAAGAGATCC-3', and reverse primer (P2) 5'-ACAGCCGAGTAGCAAGGAGG-3', which amplify 410 bp and 277 bp fragments from the floxed and the *prmt1* wild-type allele, respectively. The *Tpbpa-Cre* transgene was amplified using the common forward primer 5'-TCCAGTGACAGTCTTGATCCTTAAT-3' (P3) and two reverse primers 5'-GGCAAATTTTGGTGTACGGTCA -3' (P4) for the transgenic allele, and 5'-CTGACCGGAGGCACTCATTT-3' (P5) for the wild-type allele. The PCR products were 225 bp and 604 bp for the transgenic and the wild-type alleles, respectively.

S1.3 *Morphological analysis of placenta and embryo*

Maternal mice were sacrificed from E14 and E19 by cervical dislocation. Fetuses were harvested immediately to take pictures with a stereomicroscope (Olympus, SZ61+DP21

1

or Leica, MZFLIII+MC120HD). Placentas or fetuses were weighed, and then were genotyped.
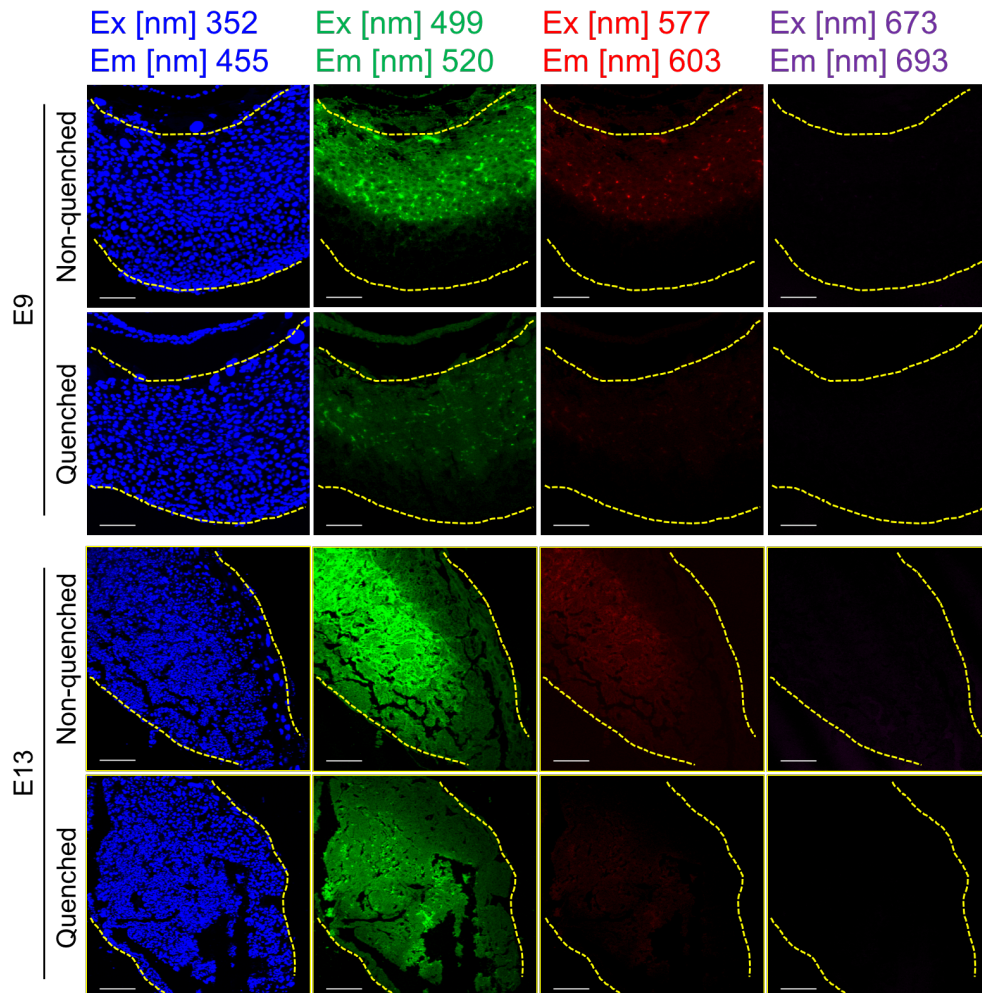
Supplementary figure

Figure 1. Immunofluorescence of sections of placenta from E9 and E13 mice. Sections were incubated with/without the TrueBlack Lipofuscin Autofluorescence Quencher. Images were obtained from the fluorescence emitted with excitation (EX) at 352 nm and emission (EM) at 535 nm (blue), EX at 499 nm and EM at 535 nm (green), EX at 577 nm and EM at 603 nm (red), and EX at 673 nm and EM at 693 nm (magenta) filters.

Supplementary figure
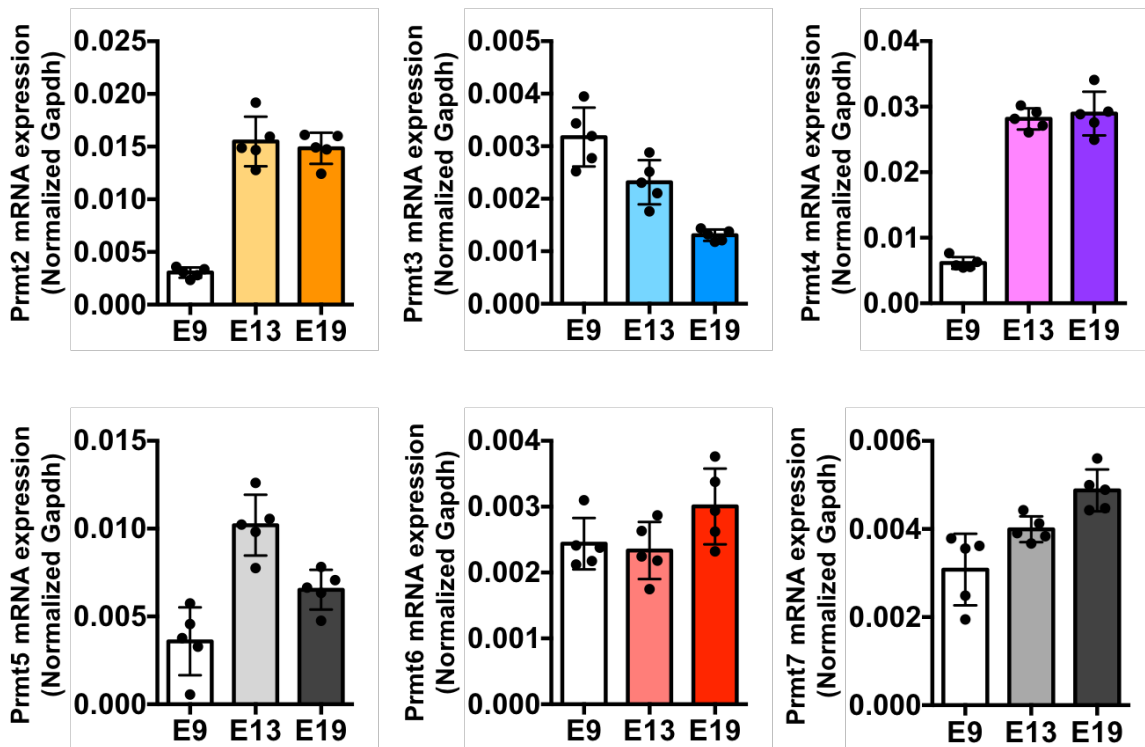
Figure 2. Altered placental expression of PRMTs in different gestational stages. Quantitative real-time PCR analysis for relative mRNA expression of placental *Prmts* (*n* = 5 per gestational stage, E9, 13 and 19).
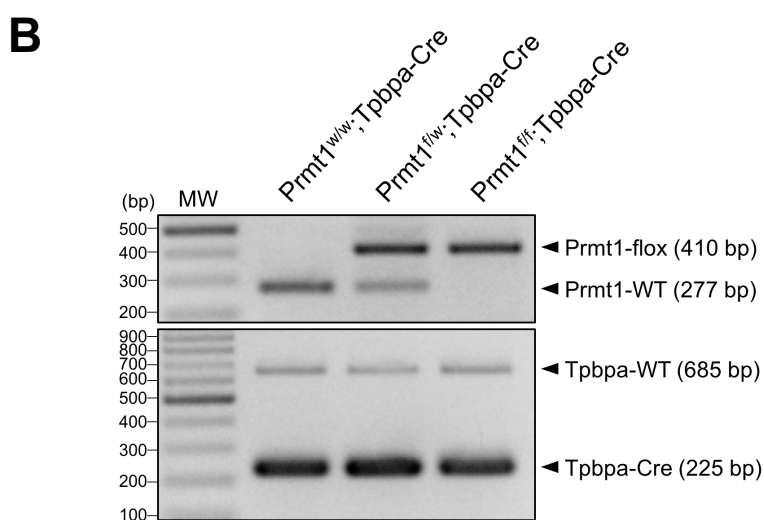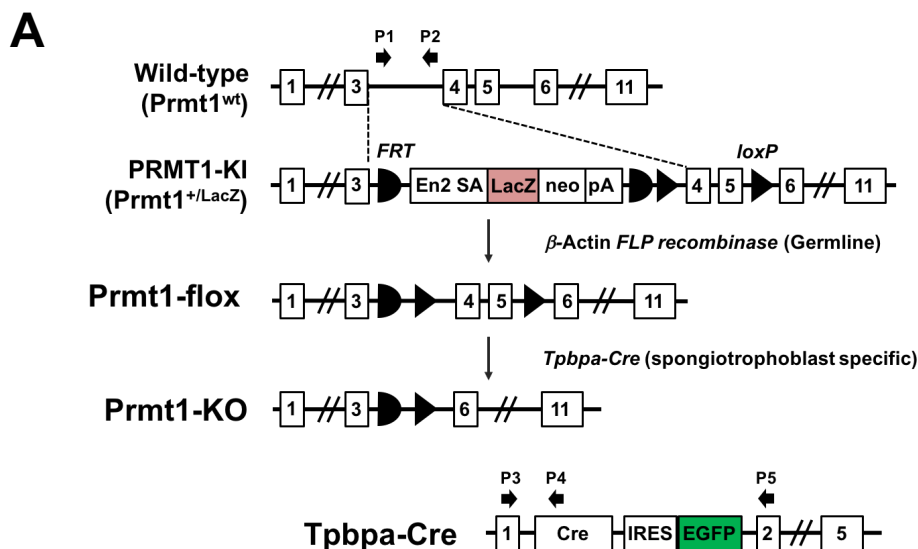
Supplementary figure

Figure 3. Generation of the junctional trophoblast-specific *Prmt1*-knockout (*Tpbpa-Cre:Prmt1*^{-/-}) mice. (A) Targeting strategy for generating *Prmt1*[f/f] mice. Top image shows the wild-type locus of the mouse *Prmt1* gene; lower images indicate constructs used for recombination; bottom image indicates Tpbpa-Cre allele. Arrows indicate the positions of the P1, P2, P3, P4 and P5 genotyping primers. **(B)** Genotyping PCR for *Prmt1* and *Tpbpa-Cre* alleles. Products of 410 and 255 base pairs (bp) were generated from Tpbpa-Cre:Prmt1 KO mice.
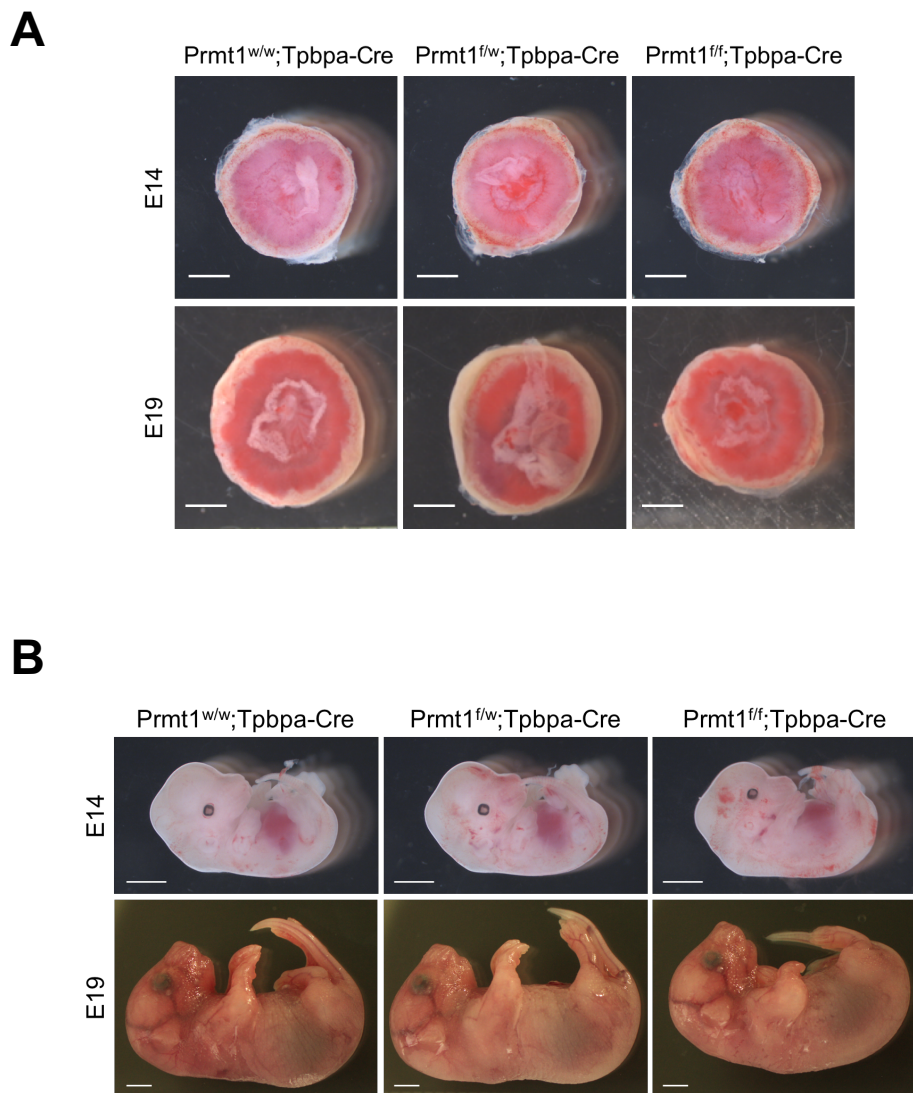
Supplementary figure

A

B

Figure 4. Gross morphologic features of placentas and embryos. (**A**) Morphologies of placenta from control (Prmt1$^{w/w}$), heterogeneous (Prmt1$^{f/w}$) and homogeneous (Prmt1$^{f/f}$) mice at E14 (upper panels) and E19 (bottom panels). Scale bars, 2 mm. (**B**) Morphologies of Prmt1$^{w/w}$, Prmt1$^{f/w}$, Prmt1$^{f/f}$ embryos at E14 (upper panels) and E19 (bottom panels). Scale bars, 2 mm.
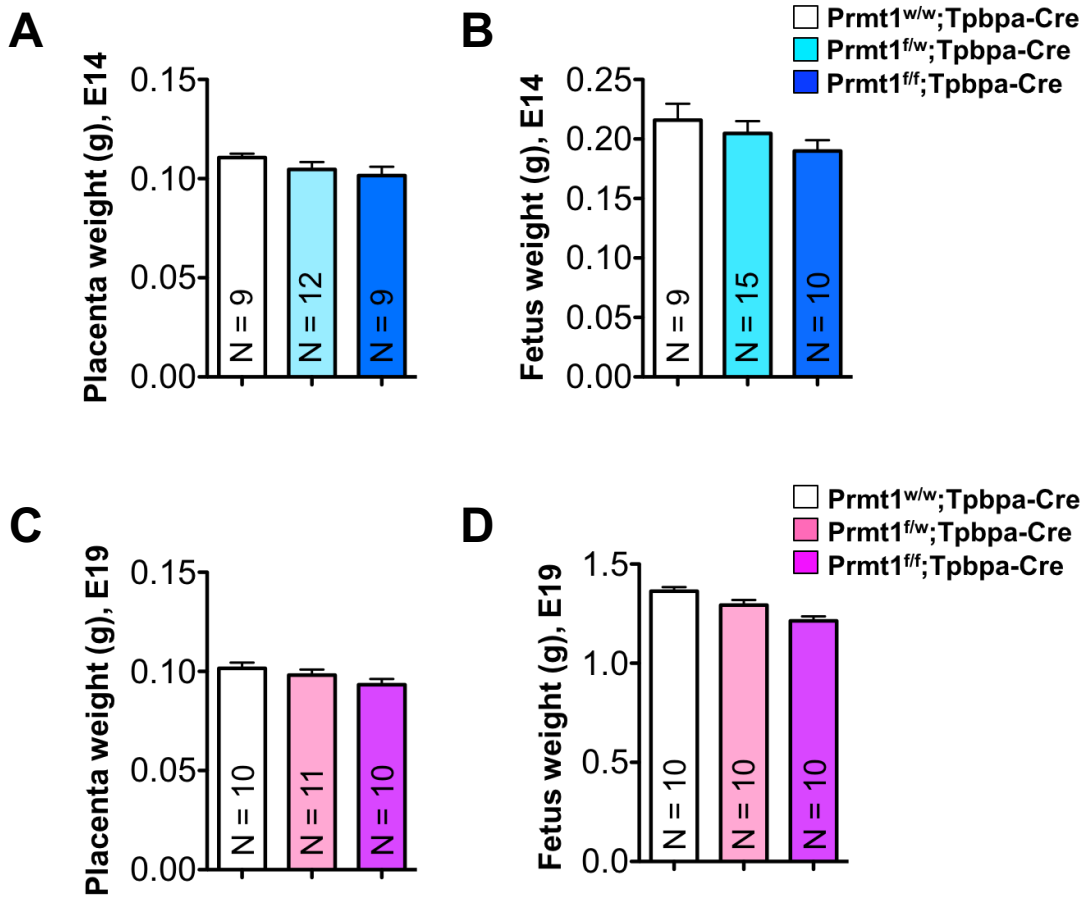
Supplementary figure

Figure 5. Average fetal and placental weights of Tpbpa-Cre:Prmt1 KO mice. (**A** and **C**) Placental weights of embryos at E14 (A) and E19 (C). Placentas were weighed subsequent to removal of umbilical cord and fetal membranes. (**B** and **D**) Fetal weights of embryos at E14 (B) and E19 (D).

Supplementary table

Table 1. The primer sequences used in qPCR.

Gene	Forward	Reverse
Prmt1	CCTCACATACCGCAACTCCA	TGGAACACTCAATCCCAATAACC
Prmt2	AATTCAGCGGAGAAACGCGG	GGGATGACCTGTGACTCGCT
Prmt3	TTACCCTGAGAACCACAAAGACG	AGTACCCAGCAACTGCCGTG
Prmt4	CATCCAGTTTGCCACACCC	GATTCCTCTGTCCGCTCAC
Prmt5	GCTTCTGGGTTCCTTTGCCG	TTCTCCAGGGATGCTCACGC
Prmt6	GAAACTGGGAGAAAGGCAAC	CACAGGTAGGCACTCAAGAC
Prmt7	AGTGCGACCTGTGTGTGACT	CAAAGGCAGACGCTACCTGG
Gapdh	TGTGTCCGTCGTGGATCTGA	TTGCTGTTGAAGTCGCAGGAG